Evaluation of the Energy Dissipation Capacities of Beam-to-Column Moment Connections for Steel Frames

Jae-Guen Yang*[1], Yong-Boem Kim[2] and Min-seok Kwak[2]

[1] Professor, Department of Architectural Engineering, College of Engineering, Inha University, South Korea
[2] Graduate Student, Department of Architectural Engineering, College of Engineering, Inha University, South Korea

Abstract

Before the occurrence of the Northridge earthquake in the United States and the southern Hyogo prefecture earthquake in Japan, beam-to-column moment connections for structural steel buildings were considered to have sufficient strength, stiffness, and energy dissipation capacities. Some of the beam-to-column moment connections demonstrated insufficient strength and energy dissipation capacities however, and suffered brittle failure when the Northridge and southern Hyogo prefecture earthquakes hit.

In South Korea, the use of beam-to-column moment connections, which are pre-qualified by some authorized architectural institutes, is strictly regulated by the Korean Building Code. In addition, the beam-to-column moment connections, which are summarized in the Standard Connection Detailing Guides published by the Korean Society of Steel Construction, can be recommended only for the application of structural steel buildings. The number of such recommended seismic resisting moment connections is limited, however, for the application of structural steel buildings. Therefore, this research was conducted to evaluate the flexural design strength and energy dissipation capacity of five connection types, and to examine their practical applicability for structural steel buildings in South Korea. Towards this end, three-dimensional nonlinear finite element analysis was conducted with respect to each of the beam-to-column moment connections.

Keywords: beam-to-column moment connections; energy dissipation capacity; flexural design strength; three-dimensional nonlinear finite element analysis

1. Introduction

The typical beam-to-column moment connections applied to steel frames include the direct-welded flange, welded flange plate, high-strength bolted flange plate, high-strength bolted double split tee, and extended end plate connections.

The direct-welded flange connection is a representative moment connection and is composed of the least member elements. The beam flange is welded onto the column flange in the form of a complete joint penetration groove weld. The shear tab is fastened onto the beam web with high-strength bolts, and welded to the column flange to support the shear force. The flange-plated connection is designed and constructed to ensure that the plate force occurring in the tension flange plate is delivered to the column member by the high-strength bolts and welds. Accordingly, the flange plate connectors, high-strength bolts, or welds should be designed to have sufficient strength to support the forces occurring between the tension flange plate and the flange. The double split tee connection fastened by high-strength bolts is applied to the case where the connection needs to be fastened onto the support member with only high-strength bolts. The connection to the beam flange takes the same form as in the flange plate connection, and the connection to the support member is treated in the same way as the tension-type connection. The extended end plate connection can take a variety of forms depending on the geometric shape of the connection. The end plate is welded onto the end of the beam member with a complete joint penetration groove weld, and then fastened to the support member with high-strength bolts on the spot. It requires a smaller number of high-strength bolts compared to other connections, and can be installed quickly. In this case, however, the tolerance of the beam member length should be small, and the end plate should be kept at a right angle. If a gap occurs between the members, the shim plate should be applied.[(1), (2), (3)] This study was conducted to evaluate the design strength and energy dissipation capacities of each connection

*Contact Author: Jae-Guen Yang, Professor,
Department of Architectural Engineering,
College of Engineering, Inha University 100 Inha-ro,
Nam-Ku, Incheon, 402-751, South Korea
Tel: +82-32-860-7588 Fax: +82-32-866-4624
(Received October 5, 2015 ; accepted July 11, 2016)
E-mail: jyang@inha.ac.kr
DOI http://doi.org/10.3130/jaabe.15.573

when the above-mentioned beam-to-column moment connections are applied to steel frames, and to review the applicability of each connection. To apply beam-to-column moment connections, which are used for the ordinary, intermediate, and special moment frame buildings, the requirements listed in Table 1. should be considered for their satisfactory performances in structural steel buildings. For this purpose, comparative analysis was performed on all the connections composed of beam and column members with the same specifications, using a three-dimensional nonlinear finite-element method.

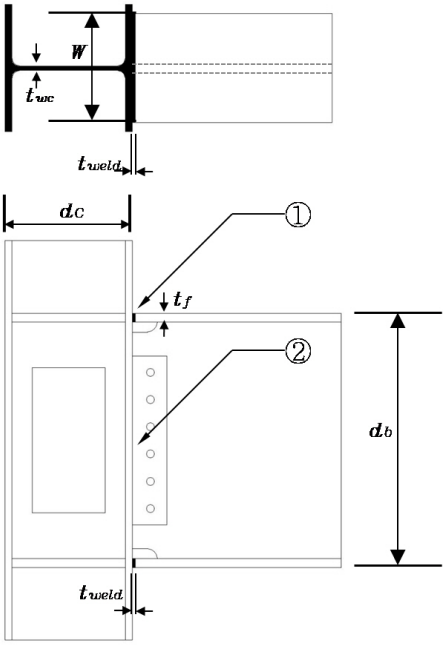

Limit states
① Beam flange-column flange weld part rupture
② Shear tab yielding; weld rupture

(a) Direct-welded flange connection

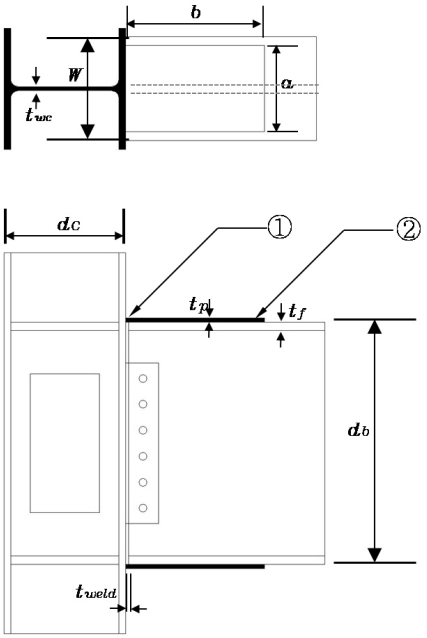

Limit states
① Beam flange-column flange weld part rupture
② Tension flange plate yielding; rupture

(b) Welded flange plate connection

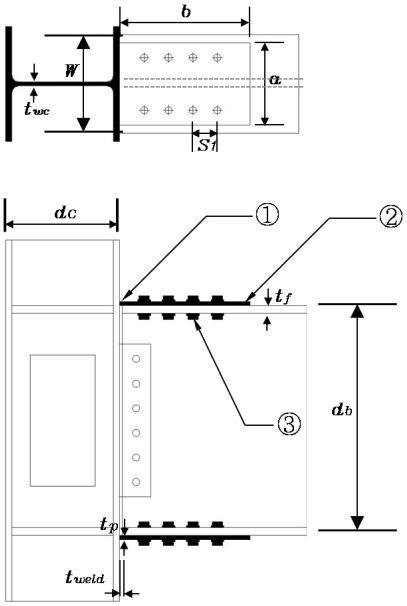

Limit states
① Tension flange plate-column flange weld rupture
② Tension flange plate yielding
③ Rupture of the high-strength bolts fastened onto the beam flange

(c) High-strength bolted flange plate connection

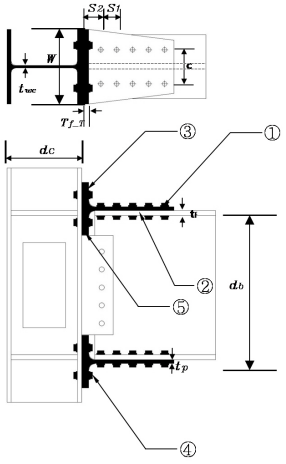

Limit states

① Rupture of the high-strength bolts fastened onto the beam flange
② Net section rupture of the T-stub stem
③ Flexural yielding of the T-stub flange
④ Tensile rupture of the high-strength bolts fastened to the T-stub flange
⑤ Net section rupture of the flange

(d) High-strength bolted double split tee connection

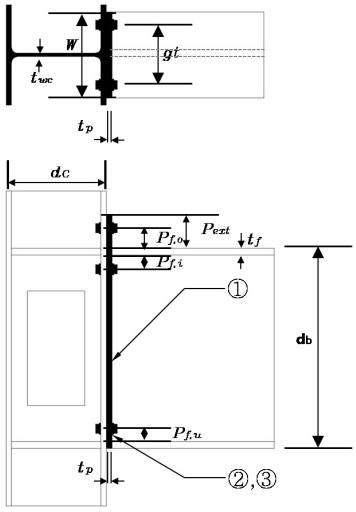

Limit states

① End plate yielding
② Tensile rupture of the high-strength bolts with no prying forces
③ Tensile rupture of the high-strength bolts with prying forces

(e) Extended end plate connection

Fig.1. Limit States and Geometric Configurations of Each Beam-to-Column Moment Connection

Table 1. Qualifying Requirements for the Flexural Strength and Total Interstory Drift of Each Moment Frame

	Required flexural strength at faying surface of the column	**Required interstory drift angular change**
Ordinary moment frame (OMF)	Over 1.1 $R_yM_{p,beam}$ for fully rigid connection/ Over 0.5 $M_{p,beam}$ for partially rigid connection	0.01
Intermediate moment frame (IMF)	Over 0.8 $M_{p,beam}$	0.02
Special moment frame (SMF)	Over 0.8 $M_{p,beam}$	0.04

2. Three-dimensional Nonlinear Finite-Element Analysis of Beam-to-Column Moment Connections

To determine the design strength of each of the beam-to-column connections applied to steel frames, the limit states of each connection were investigated, and then what provides the smallest strength value was selected. The design strengths of the high-strength bolted flange plate and double split tee connections were determined considering the limit states on the bearing and tearing as well as the shear rupture, tensile yielding and rupture, and shear-tension interaction of the high-strength bolts. The design strengths of the direct-welded flange and welded-flange-plate connections were determined considering the limit states on the shear and tensile ruptures of the welded part. In addition, the design strengths of the welded and high-strength bolted flange plate connections were determined considering the limit states of the block shear, shear rupture, shear yielding, tensile rupture, tensile yielding, and compressive buckling of the splice plate. The design strength of the shear tab connection to the web of the beam member was determined considering the limit states on the shear tab-column flange welded-part rupture, block shear, shear rupture, and shear yielding of the shear tab. In addition, the limit states of the shear rupture, shear yielding, and flexural yielding of the coped section on the beam member were considered to determine the design strength of the beam-to-column moment connections. Besides, those of the web panel zone shear, web compressive buckling, web crippling, web local yielding, and flange local bending on the column member were considered to determine the design strength of the connections.[4]

Beam-to-column moment connections applied to steel frames should be designed to have sufficient strength and appropriate energy dissipation capacities. In this study, the seismic performance of each beam-to-column moment connection was investigated by analyzing the energy dissipation capacity corresponding to the inner area of the hysteresis loop in terms of the bending moment-rotational angle

Table 2. Geometric Parameters of Each Beam-to-Column Moment Connection Model (unit: mm)

	t_f	t_{weld}	t_{wc}	t_p	α	b	S_1	S_2	t_w	T_{f_T}	c	g_t	P_{ext}	$P_{f,o}$	$P_{f,i}$	$P_{f,u}$	h_0	h_1	s
DWFC	24	8	12	-	-	-	-	-	-	-	-	-	-	-	-	-	-	-	-
WFPC	24	8	12	12	250	360	-	-	-	-	-	-	-	-	-	-	-	-	
BFPC	24	8	12	12	250	360	75	-	-	-	-	-	-	-	-	-	-	-	-
BDSTC	24	-	12	19	45	65.5-	75	103	19	37	200	210	-	-	-	-	-	-	-
UEEPC	24	-	12	20	-	-	-	-	-	-	-	-	115	70	50	50	770	622	50

relationship obtained through three-dimensional nonlinear finite-element analysis.

2.1 Three-dimensional Nonlinear Finite-element Analysis and Modeling of Beam-to-Column Moment Connections

For the analysis model of beam-to-column moment connections for steel frames, C3D8R (eight-node liner brick, reduced integration, hourglass control) of the commercial program ABAQUS (ver. 6.14) was applied as a member element. The analysis model for beam-to-column moment connections was assumed to be composed of a column member using H-350 x 350 x 12 x 19 SM490 steel, a beam member using H-700 x 300 x 13 x 24 SS400 steel, a T-stub member, a tension flange plate, and an end plate. The geometric parameters and limit states of each connection are summarized in Table 2. and Fig.1. In the finite-element analysis, nominal strength values were applied as material properties of the beam member, column member, tension flange plate, T-stub, and high-strength bolts, as summarized in Tables 3-5. F10T-M20, M30 high-strength bolts were fastened so that 165 and 371kN axial forces could be generated. The welding material was idealized using a matching electrode that had the same value as the base metal strength of each connection to be welded. In the modeling of each connection, the contact and bearing pressure between the members and the introduction of the pre-tension of the high-strength bolts were also taken into account. The slip coefficient between the members was 0.5 under the assumption that the surface would not be coated after blasting. The cyclic loading was assumed to be applied in the form of a shear force in the vertical direction to the beam end under the loading conditions presented in FEMA350, the same as in Table 6. The ABAQUS options that were applied in the finite-element analysis are summarized in Table 7.[5), (6), (7), (8), (9), (10)]

Table 3. Material Properties of Beam and Column for the Finite Element Analysis

F_y (N/mm^2)	F_u (N/mm^2)	E (N/mm^2)	ε_y	ε_u
325	490	205,000	0.001585	0.08158

Table 4. Material Properties of the Shear Tab, Stiffener, Double Plate, and Continuity Plate for the Finite Element Analysis

F_y (N/mm^2)	F_u (N/mm^2)	E (N/mm^2)	ε_y	ε_u
235	400	205,000	0.001146	0.081146

Table 5. Material Properties of the High-strength Bolt for the Finite Element Analysis

F_y (N/mm^2)	F_u (N/mm^2)	E (N/mm^2)	ε_y	ε_u
900	1,000	205,000	0.003886	0.0115854

Table 6. FEMA/SAC Loading Protocol for the Finite Element Analysis

Peak deformation	No. of cycles	Displacement (mm)
θ=0.00375 rad	6	0.0131
θ=0.005 rad	6	0.0175
θ=0.0075 rad	6	0.0262
θ=0.01 rad	4	0.0350
θ=0.015 rad	2	0.0525
θ=0.02 rad	2	0.0700
θ=0.03 rad	2	0.1050
θ=0.04 rad	2	0.1400
θ=0.05 rad	2	0.1750
θ=0.06 rad	2	0.2100

Table 7. ABAQUS Options for the Finite Element Analysis

Contact surface	Command	Option			Element type
T-stub - column	Contact	Finite sliding	Allow separation after contact	Adjust only to remove over closure	C3D8R
T-stub - beam					
T-stub - bolt					
Beam - bolt					
Column - bolt					
Other bolted parts					
Column -doubler plate	mpc	Tie			
Column -continuity plate					
Column - shear tab					
Beam - stiffener					
Other welded parts					

2.2 Results of the Three-dimensional Nonlinear Finite-element Analysis on Beam-to-Column Moment Connections

Fig.2. shows the stress distribution and deformation patterns that occurred in the connections obtained through the three-dimensional nonlinear finite-element analysis that was conducted on the beam-to-column moment connections. In the case of the direct-

welded flange connection, as the load increased, stress concentration occurred at the welded zone of the beam and column flanges, and as high-strength bolts were fastened onto the beam web, stress concentration also occurred in the shear tab welded onto the column flange, as shown in Fig.2.(a). The direct-welded flange connection suffered final failure due to the rupture of the tension-shear combination of high-strength bolts supporting the shear tab. In the case of the welded flange plate connection, as the load increased, stress concentration occurred at the welded zone where the beam flange comes in contact with the tension flange plate and at the welded zone of the tension flange plate and the column flange, as shown in Fig.2.(b). Stress concentration also occurred at the welded zone of the column flange and shear tab. The welded flange plate connection suffered final failure due to the rupture of the beam flange- tension flange plate welded zone. In the case of the high-strength bolted flange plate connection, as shown in Fig.2.(c), as the load increased, stress concentration occurred at the welded zone where the column flange comes in contact with the tension flange plate, and in the beam plate, tension flange plate, and high-strength bolt shank. Stress concentration also occurred at the column flange-shear tab welded zone. The high-strength bolted flange plate connection suffered final failure due to the rupture of the tension-shear combination of high-strength bolts supporting the shear tab. In the case of the high-strength bolted double split tee connection, as shown in Fig.2.(d), as the load increased, stress concentration occurred in the area where the T-stubs come in contact with the high-strength bolts and the T-stub fillet, and in the high-strength bolts. The high-strength bolted double split tee connection suffered final failure due to the rupture of the tension bolt in the T-stub flange. In the case of the extended end plate connection, as shown in Fig.2.(e), as the load increased, stress concentration occurred in the end plate and in the high-strength bolts. The extended end plate connection suffered final failure due to the tensile rupture of the high-strength bolts.

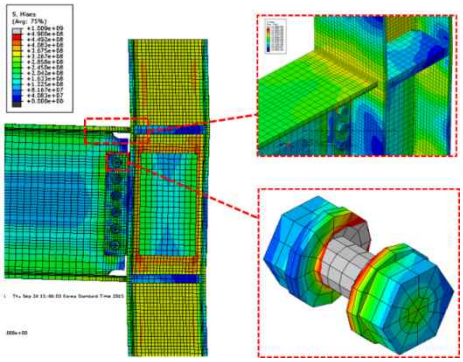

(a) Direct-welded flange connection

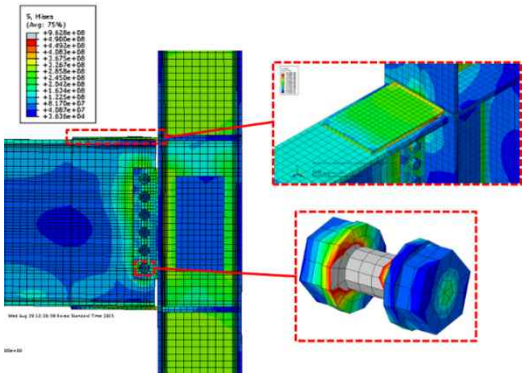

(b) Welded flange plate connection

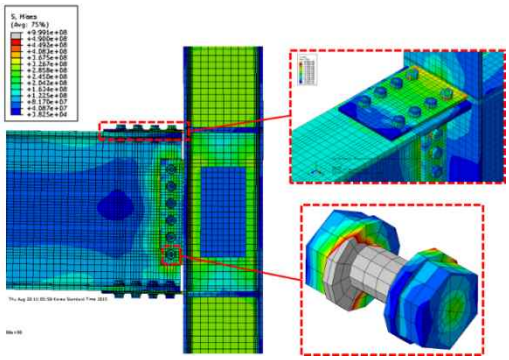

(c) High-strength bolted flange plate connection

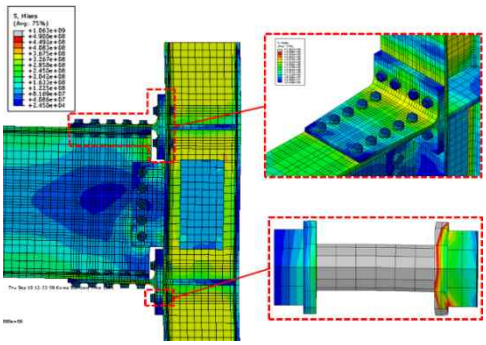

(d) High-strength bolted double split tee connection

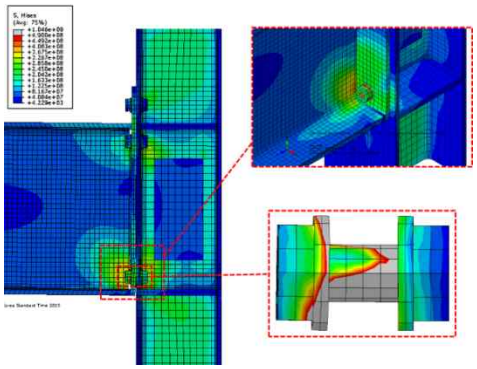

(e) Extended end plate connection

Fig.2. Stress Concentration of the Analysis Model for Beam-to-Column Moment Connections

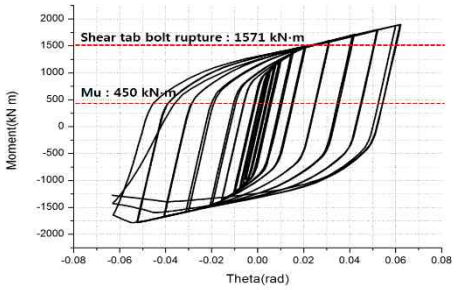

(a) Direct-welded flange connection

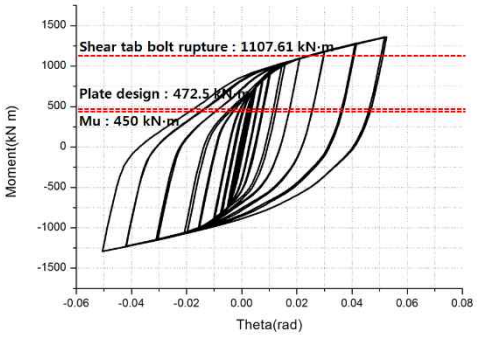

(b) Welded flange plate connection

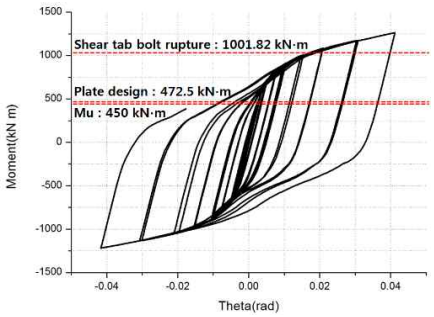

(c) High-strength bolted flange plate connection

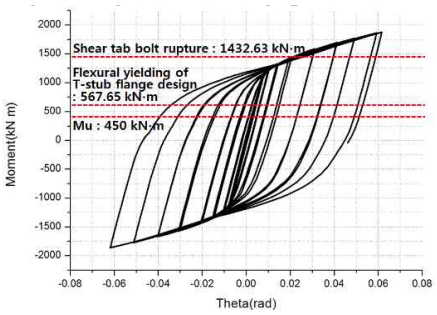

(d) High-strength bolted double split tee connection

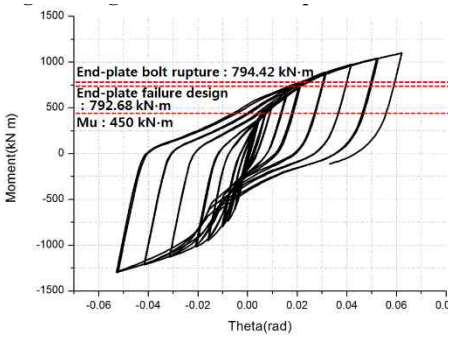

(e) Extended end plate connection

Fig.3. Hysteresis Loop Showing the Moment-rotational Angle Relationship of the Analysis Model for Beam-to-Column Moment Connections

Fig.3. shows a hysteresis loop that represents the moment-rotational angle relationship of the connections obtained through the three-dimensional nonlinear finite-element analysis that was conducted on beam-to-column moment connections. As shown in Fig.3., the beam-to-column moment connections met the required flexural strength Mu=450 kN·m and the design value for the flexural strength of each connection. Therefore, as each beam-to-column moment connection showed proper bending moment resisting strength and the corresponding stiffness, its applicability as a seismic connection is considered to be high.

3. Evaluation of the Design Flexural Strengths and Energy Dissipation Capacities

With respect to the beam-to-column moment connections, the limit states of each connection were examined, and the design strengths of the connections were calculated as summarized in Table 8. As shown in Table 8., the design strength value of each connection was located within the hysteresis loop showing the bending moment-rotational angle relationship obtained through three-dimensional nonlinear finite-element analysis. As the beam-to-column moment connections considered in this research have sufficient flexural moment resisting capacities, these connections are considered to have enough flexural strength for the applied load. Furthermore, the dimensionless energy dissipation capacity values obtained using equation (1) of each beam-to-column moment connection are listed in Table 9. As shown in such table, the dimensionless energy dissipation capacity values of each beam-to-column moment connection considered in this research are larger than those of the similar connection types commented on by Mazzolani and Piluso.[11] As such, the connections considered in this research have sufficient energy dissipation capacities for the stable structural behavior of steel buildings. Among the beam-to-column moment connections considered in this research, the direct welded flange connection provided the biggest energy dissipation capacity value,

followed by the bolted double split tee connection.

$$\overline{E} = E_{d,total} \times \frac{3EI_b}{M_{pb}^2 L} \quad (1)$$

Here,
$E_{d,total}$: Total energy dissipation capacities
E: Modulus of elasticity
I_b: Section modulus of the beam
M_{pb}: Plastic bending moment of the beam
L: Length of the column flange's surface to loading

Table 8. Limit States of the Beam-to-Column Moment Connection

Analysis model	Critical limit state	Design flexural strength values (kN·m)
DWFC	①	Determined to be full-strength
WFPC	②	472.5
BFPC	②	472.5
BDSTC	③	617.38
UEEPC	①	729.68

Table 9. Comparison of the Energy Dissipation Capacities of Beam-to-Column Moment Connections

Analysis model	$\overline{E}$
DWFC	2,140.64
WFPC	529.34
BFPC	1,054.59
BDSTC	1,118.72
UEEPC	260.83

4. Conclusion

In this study, the design strengths and energy dissipation capacities of beam-to-column moment connections applied to steel frames composed of the same beam and column members were examined. With respect to each beam-to-column moment connection, below are the conclusions that were obtained through three-dimensional nonlinear finite-element analysis.

1) As predicted, each beam-to-column moment connection suffered final failure due to the intensified stress concentration in the area where the connection member comes in contact with the welded zone, end plate, and high-strength bolts.

2) As the considered beam-to-column moment connections demonstrated sufficient design flexural strengths and energy dissipation capacities, they can be applied to intermediate moment frames.

3) Although the direct-welded flange connection exhibited the greatest energy dissipation capacity, the double split tee connection fastened with high-strength bolts was found to have higher field applicability given the ease of construction.

4) For the field application of the beam-to-column moment connections proposed in this study, there is a need not only to perform additional finite-element analysis but also to conduct experimental studies in which the proposed connection details would be applied.

Acknowledgement

This study is a summary of a part of the research findings with the support of the National Research Foundation of Korea (Project No. NRF-2013R1A2A2A07067970) and INHA University. The authors wish to express their deep gratitude to the said institutions.

List of Nomenclatures

W: Width of the column flange
t_{wc}: Thickness of the column web (mm)
t_{weld}: Thickness of the column flange-beam flange weld (mm)
d_c: Depth of the column (mm)
α: Width of the flange plate (mm)
b: Length of the flange plate (mm)
t_p: Thickness of the flange plate (mm)
t_f: Thickness of the T-stub flange (mm)
t_f': Thickness of the T-stub flange (mm)
s_1: Gauge of the distance from the high-tension bolt of the T-stub stem (mm)
s_2: Gauge of the distance from the high-tension bolt of the T-stub flange to the first high-strength bolt of the stem (mm)
g_i: Gauge of the distance from the high-tension bolt of the T-stub flange (mm)
F_y: Yield strength of the steel (N/mm^2)
F_u: Ultimate strength of the steel (N/mm^2)

References

1) Geschwindner, L. F., Unified Design of Steel Structures, John Wiley & Sons, INC., 2008.
2) Salmon, C. and Johnson, J. (2005) Steel Structures, Design and Behavior, 5th Ed., Harper & Row.
3) AISC, (201) Load and Resistance Factor Design Specification for Structural Steel Buildings, 14th Ed., American Institute of Steel Construction, Chicago, IL.
4) FEMA (2000) "Recommended Seismic Design Criteria for New Steel Moment-Frame Buildings", Program to Reduce the Earthquake Hazards of Steel Moment Frame Structures, FEMA 350, Federal Emergency Management Agency, Washington, D.C.
5) Yang, J. G., Park, J. H., Choi J. H. and Kim, S. M. (2011) Characteristic Behavior of a T-stub Connection Under Shear, Including the Effects of Prying Action and Bolt Pretension, The 6th International Symposium on Steel Structures, KSSC, Korea, pp.1086-1092.
6) Yang, J. G., Kim, H. K. and Park, J. H. (2012) Analytical Models for the Initial Axial Tensile Stiffness and Ultimate Tensile Load of a T-Stub, Including the Effects of Prying Action, International Journal of Steel Structures, KSSC, Vol. 24, No. 3, pp.279-287.
7) Kim, H. D., Yang, J. G., Lee, Jae. Yun. and Lee, H. D. (2014) Evaluation of the Initial Rotational Stiffness of a Double Split Tee Connection, Including the Effects of Prying Action, International Journal of Steel Structures, KSSC, Vol. 26, No. 2, pp.133-142.
8) Piluso, V., Faella, C. and Rizzano, G. (2001) Ultimate Behavior of Bolted T-stubs. I: Theoretical Model, Journal of Structural Engineering, ASCE, Vol. 127, No. 6, pp.686-693.
9) Swanson, J. A., Ko, Kan, D. S. and Leon, R. T. (2002) Advanced Finite Element Modeling of Bolted T-stub Connection Components, Journal of Constructional Steel Research, Elsevier, Vol. 58, No. 5, pp.1015-1031.
10) Lemonis, M. E. and Gantes, C. J. (2006) Incremental Modeling of T-Stub Connections, Journal of Mechanics of Materials and Structures, Vol. 1, No 7, pp.1135-1159.
11) Mazzolani, F. M. and Piluso, V. (1996) Theory and Design of Seismic Resistant Steel Frames. E & F N SPON, pp.285-304.